A Conserved Motif in the Tail Domain of Vinculin Mediates Association with and Insertion into Acidic Phospholipid Bilayers†

Robert P. Johnson,‡ Verena Niggli,§ Peter Durrer,|| and Susan W. Craig*,‡,⊥

Departments of Biological Chemistry and Pathology, Johns Hopkins School of Medicine, Baltimore, Maryland 21205, Department of Pathology, University of Bern, CH-3010 Bern, Switzerland, and Department of Biochemistry, Swiss Federal Institute of Technology (ETH), CH-8092 Zürich, Switzerland

Received November 3, 1997; Revised Manuscript Received March 31, 1998

ABSTRACT: The tail domain of vinculin (V_t) contains a salt-insensitive binding site for acidic phospholipids which is masked by the intramolecular head−tail interaction in native vinculin [Johnson, R. P., and Craig, S. W. (1995) *Biochem. Biophys. Res. Commun. 210*, 159−164]. To characterize further this phospholipid binding site, we have used hydrophobic photolabeling with a photoactivatable phosphatidylcholine analogue to detect insertion of protein into the lipid bilayer. We show here that, although the properties of binding to acidic phospholipid vesicles and spontaneous insertion into the bilayer are cryptic and inactive in vinculin at physiologic ionic strength, these activities of the purified tail domain can be activated by physical and chemical disruption of the intramolecular interaction between the head and tail domains. By analyzing the lipid binding and insertion activity of a series of GST−V_t fusion proteins, we defined 55 amino acids, comprising vinculin residues 916−970, that mimic the lipid-binding and insertion activity of V_t. Predictions of secondary structure suggest that these 55 amino acids form a basic, amphipathic helical hairpin. This prediction is supported by circular dichroism analysis, which indicates that at least 80% of the residues in residues 916−970 are in a helical conformation. This predicted helical hairpin motif, which is conserved in all vinculins and is present in an acidic phospholipid-binding region of α-catenin, is distinct from C2 and PH domains, and likely represents a third type of acidic phospholipid-binding structure.

Vinculin is a modular protein (*1*) with separate binding domains for α-actinin, talin, actin, VASP, and acidic phospholipids (*2*). During various cellular activities, vinculin is recruited from the cytoplasm to cell membrane adhesion sites where it has roles in regulating cell adhesion, spreading, and motility (*3*). Many of the ligand-binding activities of purified vinculin are inhibited by a high-affinity intramolecular interaction between the head and tail domains of vinculin (*4*−*9*). Because acidic phospholipids affect the activity of several cytoskeletal and signaling proteins (*10*−*12*), it is potentially important that, in buffers with low ionic strengths, vinculin associates with acidic phospholipids (*6*, *13*, *14*), major components of the cytoplasmic leaflet of eukaryotic plasma membranes (*15*). Although the sensitivity of this interaction to physiologic ionic strength (*6*, *13*, *14*) would not support its in vivo significance, vinculin can be labeled by photoactivatable phospholipid analogues incorporated into lipid bilayers both in vitro (*14*) and in vivo (*16*).

Vinculin is cleaved by *Staphylococcus aureus* V8 protease to produce an amino-terminal 95 kDa head domain and a carboxyl-terminal 30 kDa tail domain (*17*, *18*), which associate intramolecularly in the native protein (*4*). Isolated tail fragment contains a salt-resistant binding site for acidic phospholipids that is masked by the head−tail interaction in native vinculin (*6*). Because native vinculin binds poorly to acidic phospholipids in buffers with physiologic ionic strengths (*6*, *13*, *14*), we proposed that regulated exposure of this phospholipid-binding site in a cell might play a role in recruitment or retention of vinculin at the plasma membrane. Interaction of vinculin with membrane phospholipids, directed by unmasking of the acidic phospholipid-binding site on the protein, could stabilize vinculin's localization at the plasma membrane and facilitate its interaction with other junctional components. Association of vinculin with the membrane could lead to partial insertion of the protein into the lipid bilayer (*14*, *16*), possibly strengthening the connection between the cytoplasmic adhesion complex and the plasma membrane.

Another potential functional consequence of vinculin−phospholipid binding is suggested by evidence that acidic phospholipids (PS, PIP, and PIP_2)[1] presented in the form of mixed Triton micelles (*8*) or of sonicated vesicles (presumably SUVs) or pure PIP_2 micelles (*9*) disrupt the regulatory

† This work was supported by the Swiss National Foundation for Scientific Research (V.N. and Dr. J. Brunner, ETH, Zürich, Switzerland) and by NIH Grant R01-GM 41605 (to S.W.C.).

‡ Department of Biological Chemistry, Johns Hopkins School of Medicine.

§ University of Bern.

|| Swiss Federal Institute of Technology.

⊥ Department of Pathology, Johns Hopkins School of Medicine.

[1] Abbreviations: PIP_2, phosphatidylinositol 4,5-bisphosphate; PS, phosphatidylserine; PI, phosphatidylinositol; PC, phosphatidylcholine; [^{125}I]TID-PC/16, 1-palmitoyl-2-[decanedioylmono[2-[^{125}I]iodo-4-(3-trifluoromethyl)-3*H*-diazirin-3-ylbenzyl]ester]-*sn*-glycerophosphocholine; GST, glutathione *S*-transferase; BME, *β*-mercaptoethanol; EDTA, (ethylenedinitrilo)tetraacetic acid; EGTA, [ethylenebis(oxyethylenenitrilo)]tetraacetic acid; PMSF, phenylmethanesulfonyl fluoride; TFE, trifluoroethanol; MLV, multilamellar vesicle; SUV, small unilamellar vesicle.

S0006-2960(97)02724-4 CCC: $15.00
Published on Web 06/23/1998

interaction of vinculin's head and tail domains in vitro, exposing binding sites for actin and talin, as well as sites for phosphorylation. The activation of vinculin's ligand binding sites observed in these studies suggests that vinculin associates with these phospholipids under the physiologic ionic conditions used in vitro, although in neither study was lipid binding to vinculin examined directly, in the absence of talin or actin.

Activation of vinculin should allow a specific structural determinant in the tail domain to serve as a membrane anchor under physiologic conditions. To test the feasibility of this idea, we have examined the structural requirements and ionic strength dependence for cosedimentation of vinculin and vinculin tail domain with acidic phospholipids, and for insertion of these proteins into the hydrophobic core of the bilayer. Our results indicate that under physiologic conditions in vitro vinculin must be in an open conformation, with the head domain displaced from the tail, before it can bind and penetrate into bilayers containing acidic phospholipids. When driven into an open conformation, vinculin associates with phospholipid bilayers through a motif in the tail domain that is conserved throughout the vinculin/α-catenin family. Analysis of the sequence of this region suggests a structural basis for the observed lipid-binding properties of vinculin and distinguishes the phospholipid-binding site in vinculin from a number of phospholipid-binding domains characterized in other proteins.

EXPERIMENTAL PROCEDURES

Phospholipids. Pure phospholipids were purchased from Avanti Polar Lipids (Alabaster, AL) or from Lipid Products (South Nutfield, Surrey, England) and stored at −20 °C in chloroform under N_2. The photoactivatable phosphatidylcholine analogue [^{125}I]TID-PC/16 [1-palmitoyl-2-[decanedioylmono[2-[^{125}I]iodo-4-(3-trifluoromethyl)-3*H*-diazirin-3-ylbenzyl]-ester]-*sn*-glycerophosphocholine] was prepared as described (*19*) to a specific activity of 2×10^3 Ci/mmol.

Protein Purification. Chicken smooth muscle vinculin and its *S. aureus* V8 protease fragments were purified as described (*4*, *18*, *20*, *21*) and stored in 10 mM Tris-HCl (pH 7.5), 1 mM EGTA, 0.1 mM EDTA, 3 mM NaN_3, 150 mM NaCl, 0.1% β-mercaptoethanol (BME), and 2× protease inhibitor cocktails I and II. A 1000× protease inhibitor cocktail (PIC) stock contained 1 mg/mL leupeptin, 2 mg/mL antipain, 10 mg/mL benzamidine, 10 KIU/mL aprotinin in H_2O (1000× PIC I) or 1 mg/mL chymostatin, and 1 mg/mL pepstatin in dimethyl sulfoxide (1000× PIC II).

GST Fusion Proteins. Construction of the GST−tail fusion proteins GST−V884−1066 and GST−V884−927 has been described (*4*). All other fusion proteins were constructed by polymerase chain reaction amplification of the appropriate region of the chicken embryo vinculin cDNA (*22*) using in-frame primers. Amplified products were ligated into the Invitrogen (San Diego, CA) pCR2.1 vector essentially according to the manufacturer's instructions, except that recombinants were transformed into competent *Escherichia coli* DH5α cells. Recombinant plasmids were digested with *Eco*RI to yield insert fragments containing the specific PCR-amplified vinculin coding region and flanking vector sequence, which were gel-purified using the Bio-Rad (Hercules, CA) Prep-a-Gene matrix and ligated into the *Eco*RI site of the GST fusion protein expression vector pGEX2T (*23*) to yield the plasmid encoding the corresponding GST−tail fusion protein. This strategy of amplification using an in-frame sense primer in the polymerase chain reaction with intermediate subcloning into pCRII always results in ligation of the *Eco*RI fragment containing the amplified sequence into pGEX2T in-frame with the GST coding region. A linker region (LVPRGSPGIPL, one-letter amino acid code) containing a thrombin cleavage site was present between GST and the fused vinculin sequence in all constructs. Vector DNAs encoding the GST fusion constructs were sequenced using Sequenase (Amersham, Arlington Heights, IL). Fusion proteins were purified as described (*4*, *23*), dialyzed against 10 mM Tris-HCl (pH 7.5), 1 mM EGTA, 0.1 mM EDTA, 3 mM NaN_3, 150 mM NaCl, 0.1% BME, 20% sucrose, and 2× PICs I and II, and stored frozen at −20 °C. GST was quantified spectrophotometrically ($E_{1cm}^{1\%} = 20$) at 280 nm (*23*). Fusion proteins were quantified using the Bio-Rad protein assay reagent using GST as the standard.

Phospholipid Cosedimentation Assay. Large, multilamellar vesicles were prepared essentially as described (*24*). Briefly, dried phospholipid films were swollen at 5 mg/mL in 20 mM Hepes (pH 7.4) and 0.2 mM EGTA for 3 h at 42 °C (*25*). The vesicles were then centrifuged (20000*g* for 20 min at 4 °C), and the pellet was resuspended in the same buffer at 5 mg/mL. Phospholipid concentrations were determined by organic phosphate analysis using the method of Ames (*26*). Fusion proteins were diluted into 20 mM Tris-HCl (pH 7.4), 0.2 mM EDTA, and 0.1% BME and incubated (30 min at 25 °C) with phospholipid vesicles (0.5 mg/mL). After dilution, the final concentration of NaCl from the fusion proteins storage buffer was 15 mM. In experiments at higher ionic strengths, the reaction mixtures also contained 80 mM KCl. After incubation, reaction mixtures were centrifuged (40000*g* for 10 min at 25 °C) in a Beckman Airfuge. Pellet and supernatant fractions were subjected to SDS−polyacrylamide gel electrophoresis (*27*) and proteins detected by Coomassie Brilliant Blue staining of the gels. The amount of GST−V884−1066 cosedimenting with PS vesicles did not vary over a range of PS concentrations (0.06−0.5 mg/mL).

Freeze−Thaw Assembly of Vinculin−Phospholipid Proteoliposomes. Vinculin−phospholipid complexes were generated by rapid freezing and thawing of codispersions of protein and lipid, by following a procedure used to study the interaction of talin with lipids (*28*). Small unilamellar vesicles were prepared by resuspension of dried phospholipid in 10 mM Tris-HCl (pH 7.5) followed by sonication (15−30 min at 25 °C) in a Branson bath sonicator at the highest power setting until a clear lipid solution was obtained. Vinculin or control proteins in 10 mM Tris-HCl (pH 7.5), 1 mM EGTA, 0.1 mM EDTA, 3 mM NaN_3, and 0.1% BME were mixed with sonicated phospholipid vesicles as indicated in the figure legends. Protein−lipid mixtures were subjected to five cycles of rapid freezing in liquid N_2 followed by thawing in a room-temperature water bath. Proteolipid complexes were then recovered by low-speed (12000*g* for 15 min) centrifugation at 4 °C. Pellet and supernatant fractions were analyzed by SDS−PAGE and Coomassie Blue staining. In the experiment depicted in Figure 2b, protein was quantified by excision of the vinculin bands from the

gel, extraction of the Coomassie Blue in H_2O−pyridine (3:1, v:v), and measurement of the extracted absorbance at 605 nm. The background signal, quantified by extracting gel slices from areas devoid of protein, was determined and subtracted.

Hydrophobic Photolabeling. Hydrophobic photolabeling using large, multilamellar liposomes was carried out essentially as described (*24*), with some modifications. PS (5 mg/mL) vesicles with 0.0005−0.0015% (w:w of total lipid) [^{125}I]TID-PC/16 ($1-3 \times 10^5$ cpm per microgram of total lipid) were prepared in 20 mM Hepes (pH 7.4) and 0.2 mM EGTA as described above. Proteins in 10 mM Tris-HCl (pH 7.5), 1 mM EGTA, 0.1 mM EDTA, 3 mM NaN_3, 150 mM NaCl, 0.1% BME, 10% sucrose, and 2× PICs I and II were diluted into a buffer containing 10 mM Hepes, 10 mM Tris-HCl (pH 7.4), 0.1 mM EGTA, 0.05 mM EDTA, and 7.5 mM BME. After dilution, the final concentration of NaCl was ≤15 mM. Proteins were preincubated (15 min at 22 °C) in the absence of liposomes, followed by the addition of liposomes (0.08−0.5 mg/mL final concentration) and a further incubation for 15 min. The relative labeling of the different proteins was independent of the total lipid concentration over this range. Some experiments were carried out with the addition of 80−90 mM KCl, as indicated. Samples were photolyzed for 4 min using a mercury lamp (HBO 200W/4, Zeiss Instruments) with a saturated solution of copper sulfate (20 mm) as a filter. Protein−lipid mixtures were subjected to SDS−PAGE and autoradiography. For quantitative evaluation of labeling, protein-containing slices were cut out from dried Coomassie Blue-stained gradient gels, placed into plastic tubes, and counted in an LKB 1272 Clinigamma counter.

His-Tag Fusion Proteins. Sequences encoding vinculin residues 884−1066 and 916−970 were amplified by polymerase chain reaction and subcloned into pCR2.1 as described above, except that amplifying primers were used which intoduced 5′-*Nde*I and 3′-*Xho*I recognition sites flanking the vinculin sequences. The amplified vinculin sequences were liberated by digestion with *Nde*I and *Xho*I, gel-purified, and ligated into the *Nde*I−*Xho*I-cleaved pET15b His-tag fusion protein expression vector (Novagen, Madison, WI). DNA constucts were sequenced with Sequenase. The His-tag fusions of V884−1066 and V916−970 were expressed in *E. coli* BL21(DE3) cells (Novagen) and purified over His-Bind Ni^{2+} chelating resin (Novagen) according to the manufacturer's instructions. The His-tag leader peptides were cleaved using the Thrombin Cleavage Capture Kit (Novagen) and removed on His-Bind resin. The resulting V884−1066 and V916−970 polypeptides have two additional N-terminal residues (histidine and methonine) not present in the vinculin primary structure, which were left over from the thrombin recognition sequence encoded in the pET15b vector.

Circular Dichroism Spectroscopy. V884−1066 and V916−970, produced from His-tag fusions by thrombin cleavage, and horse heart myoglobin (Schwarz-Mann Biotech, Cleveland, OH), were dialyzed extensively against circular dichroism (CD) buffer [10 mM sodium phosphate (pH 7.0), 100 mM NaCl, 1 mM EDTA, 0.1 mM EGTA, 3 mM NaN_3, and 0.5 mM BME]. The concentration of V884−1066 was determined both spectrophotometrically, using a calculated extinction coefficient at 280 nm of 18 710 M^{-1} cm^{-1} (29), and by BCA protein assay (Pierce, Pockford, IL) using bovine serum albumin as a standard; the values determined by the two methods were within 10% of each other. The concentration of V916−970, which contains no tryptophan or tyrosine residues, was determined by BCA. The myoglobin concentration was determined spectrophotometrically at 280 nm using the published value for $E_{1cm}^{1\%}$ of 17.9 (*30*). CD spectra were recorded on an AVIV 60 Spectropolarimeter (AVIV, Lakewood, NJ) at 0.5 nm intervals over the 185−260 nm wavelength range, using 0.20−0.22 mg/mL protein in CD buffer in a 0.1 mm path length cell (Hellma Cells, Jamaica, NY). Five to seven scans were recorded for each sample and averaged. The protein spectra were corrected by subtraction of the spectrum of CD buffer, and the corrected protein spectra were adjusted for protein concentration and path length to obtain the mean residue ellipticity at each wavelength. The data were smoothed using AVIV 60 software. Calibration of the spectropolarimeter was confirmed by measurement of the spectrum of (+)-10-camphorsulfonic acid (*31*). In one experiment, 100% TFE was added to V916−970 to yield final concentrations of 10−40%; an aliquot of a concentrated stock of the CD buffer was also added to adjust for the volume of TFE. The protein spectra at each TFE concentration were corrected by subtraction of the spectrum of buffer containing the appropriate concentration of TFE. TFE and (+)-10-camphorsulfonic acid were obtained from Aldrich Chemicals (Milwaukee, WI).

RESULTS

Binding of Vinculin and Its Tail Domain to Multilamellar Vesicles: Characterization of Ionic Strength Sensitivity and Phospholipid Selectivity. The purified 30 kDa tail fragment cosediments with multilamellar vesicles (MLVs) composed of phosphatidylserine (PS) in both low- and high-ionic strength buffers, whereas intact vinculin cosediments with acidic phospholipids only in low (0−15 mM salt)-ionic strength buffers (Figure 1a,b). The designation "0 mM salt" refers to solutions buffered with Hepes or Tris and metal chelators (EDTA and EGTA) and containing only those amounts of salt introduced by adjusting the pH with NaOH and HCl. These results are consistent with those from gel filtration assays, in which vinculin binds weakly ($K_d \sim 5$ μM) to large unilamellar vesicles composed of acidic phospholipids in very low-ionic strength (no salt) buffers (*6*) and with other studies showing that vinculin binding to acidic phospholipids is extremely sensitive to salt concentration (*13*, *14*). In buffers lacking monovalent salt, vinculin shows a preference for MLVs composed of PI (phosphatidylinositol) and PIP_2 (phosphatidylinositol 4,5-bisphosphate) over PS, but this preference, as well as lipid binding itself, is nearly abolished at 15 mM salt (Figure 1b). Both the gel filtration experiments (*6*) and the cosedimentation assays reported here show that, in contrast to intact vinculin, the carboxyl-terminal tail domain binds tightly to acidic phospholipids in a relatively salt-insensitive manner (Figures 1a and 4).

Hydrophobic Photolabeling To Assay Insertion of Vinculin and Its Tail Domain into the Hydrophobic Core of Acidic Phospholipid Bilayers. Hydrophobic photolabeling experiments also differentiate the interaction of vinculin and the free 30 kDa tail domain with acidic phospholipid vesicles. When incorporated into PS vesicles, [^{125}I]TID-PC/16, a

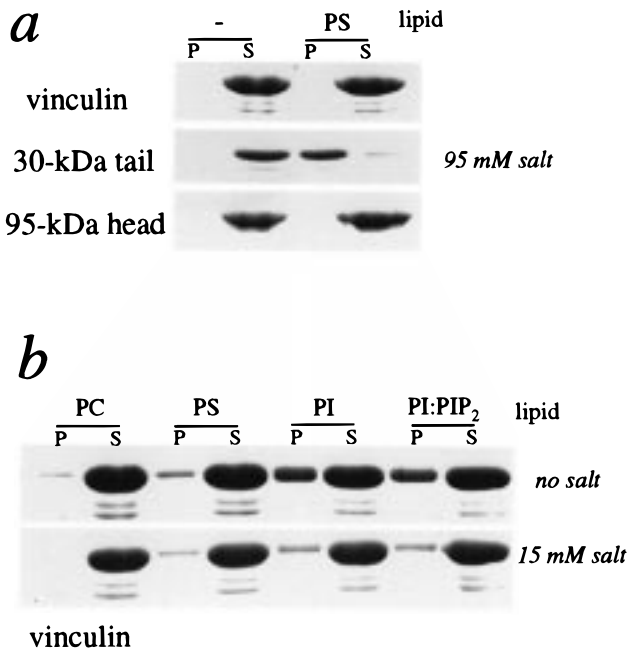

FIGURE 1: Vinculin 30 kDa tail fragment binds more tightly to acidic phospholipid vesicles than does native vinculin. (a) Vinculin (2 μM) or its 30 kDa tail fragment (4 μM) or 95 kDa head fragment (2 μM) was incubated (30 min at 25 °C) with multilamellar PS vesicles (0.5 mg/mL) in low-ionic strength buffer (see Experimental Procedures) containing 15 mM NaCl and 80 mM KCl (total, 95 mM salt). PS vesicles were sedimented, and pellet (P) and supernatant (S) fractions were analyzed by SDS−PAGE and Coomassie Blue staining. (b) Vinculin was incubated with vesicles composed of various phospholipids as indicated, in buffer containing no added salt or containing 15 mM NaCl. The molar ratio of PI:PIP_2 was 1:1.

Table 1: Hydrophobic Photolabeling of Vinculin and Vinculin Fragments[a]

		^{125}I incorporated (cpm/nmol of protein)		
photolysis	KCl	vinculin	95 kDa head	30 kDa tail
−	−	165	nd	65, 210
−	+	nd	nd	221, 317
+	−	159 ± 84	208 ± 166	1688 ± 277
+	+	nd	nd	633 ± 154

[a] Purified vinculin (1.3 μM), 95 kDa head (1.6 μM), or 30 kDa tail (3 μM) was incubated with large phosphatidylserine liposomes containing trace amounts of [^{125}I]TID-PC/16 in the presence of 11.2 mM NaCl with or without additional 90 mM KCl as indicated, followed by photolysis, SDS−PAGE, and determination of radioactivity incorporated into the protein bands. Background radioactivity measured in the same lane (40−60 cpm per lane) was always subtracted from that measured in the bands. Aliquots of reaction mixtures were applied to the gels corresponding to 105 pmol of tail, 35 pmol of vinculin, and 56 pmol of head. The background radioactivity was measured in a gel slice of the same size of the protein band and obtained from the same lane (40−60 cpm per slice) and was subtracted from that measured in the bands. Signal:background counts per minute ratios equal to or greater than 2 are considered significant. Incorporated radioactivity in counts per minute per nanomole of protein is indicated as the mean ± standard deviation (SD) of three or four experiments (nd, not determined). The values for background labeling of vinculin and 30 kDa tail in the absence of photolysis represent the results of single or duplicate determinations.

photoactivatable analogue of phosphatidylcholine, reacts covalently with the 30 kDa tail domain in a photolysis-dependent manner (Table 1). Very little or no specific labeling of vinculin was detected under these experimental conditions (11.2 mM salt), although photolabeling of vinculin in the presence of acidic phospholipids and the absence of salt was established in earlier studies (*14*). The amino-terminal 95 kDa head domain does not insert into phospholipid bilayers under the conditions used in this study (Table 1). Because the photoactivatable moiety of [^{125}I]TID-PC/16 is attached to the C10 position of one of the fatty acyl chains, and thus is buried in the hydrophobic core of the phospholipid bilayer, photolabeling by this reagent indicates partial insertion of the labeled protein into the acyl region of the bilayer, most likely through hydrophobic amino acid side chains (*32*).

Properties of Vinculin−Lipid Complexes Formed by Freezing and Thawing. Our results indicate that native vinculin is precluded from spontaneously associating with or inserting into acidic phospholipid MLVs under physiologic conditions. In contrast, native vinculin can be driven to associate with acidic phospholipids by cycles of freezing and thawing (freeze−thaw), a procedure used to study talin−phospholipid interaction (*28*) and to reconstitute activity of purified membrane proteins (*33*). During freeze−thaw in the presence of acidic phospholipid (PI) vesicles in buffer lacking salt, vinculin is incorporated almost quantitatively into low speed-sedimentable proteolipid complexes, whereas little to no incorporation occurs with neutral phospholipid (PC, phosphatidylcholine) vesicles (Figure 2a). No significant incorporation of bovine serum albumin is observed with either acidic or neutral phospholipid (Figure 2a). Other control proteins such as ovalbumin and carbonic anhydrase also failed to be incorporated into proteolipid complexes, whereas vinculin formed complexes with PS as well as with PI vesicles (data not shown). PI-incorporated vinculin can be completely digested by proteinase K, demonstrating that vinculin is associated with the surface of the lipid vesicles and not merely trapped inside them during freeze−thaw (Figure 2a). Digestion of PI-incorporated vinculin with *S. aureus* V8 protease yields discrete fragments (Figures 2a and 3), indicating that vinculin incorporated into PI vesicles via freeze−thaw retains its overall folded structure, and is not simply denatured at the surface of the lipid bilayer. Formation of vinculin−lipid complexes during freeze−thaw is dependent upon the composition of the lipid vesicles. The extent of vinculin incorporation into mixed PI−PC vesicles increases as the percentage of acidic phospholipid increases (Figure 2b). Thus, vinculin displays the same preference for acidic phospholipids during freeze−thaw as observed when vinculin−phospholipid binding is analyzed by gel filtration (*6*, *13*) or hydrophobic photolabeling (*14*).

The extent of vinculin incorporation also depends on the ionic strength of the medium (Figure 2b). However, significant incorporation during freeze−thaw is observed even at high ionic strengths (150 mM NaCl), a condition under which, in the absence of freeze−thaw, very little to no vinculin−lipid binding can be detected by gel filtration (*6*) or cosedimentation assays. Hydrophobic photolabeling of native vinculin increases approximately 14-fold following freeze−thaw incorporation into PS vesicles (Figure 2c). Vinculin must be present with the lipid during freeze−thaw to observe this increase in photolabeling; if the PS vesicles are subjected to freeze−thaw before addition of vinculin, no greater labeling of the protein occurs than when vinculin and vesicles are incubated without freeze−thaw (Figure 2c).

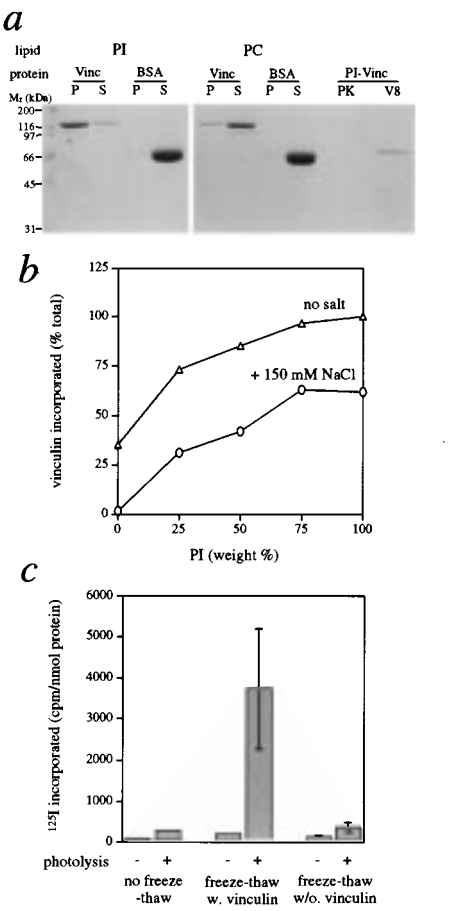

FIGURE 2: Vinculin is incorporated into acidic phospholipid vesicles during freeze−thaw, and its labeling by hydophobic probe is greatly enhanced. (a) Vinculin (3 μM) or BSA (6 μM) in 10 mM Tris-HCl (pH 7.5), 1 mM EGTA, 0.1 mM EDTA, 3 mM NaN_3, and 0.1% BME was mixed with sonicated vesicles composed of PI or PC (3 mM lipid) and the mixture subjected to five cycles of freeze−thaw. Samples were centrifuged (12000*g* for 15 min at 4 °C) to separate lipid vesicles with protein incorporated (pellet, P) from unincorporated protein (supernatant, S), and aliquots of these fractions were analyzed by SDS−PAGE. Aliquots of PI-incorporated vinculin, resuspended in buffer, were also incubated with 10 μg/mL proteinase K (PK) or with 40 μg/mL protease V8 (V8) before SDS−PAGE to demonstrate that PI-incorporated vinculin is accessible on the surface of the liposomes and retains V8 protease-resistant structure. (b) Sonicated PI−PC vesicles (1 mM total lipid) containing the indicated weight percent of PI were mixed with vinculin (1 μM) in 10 mM Tris-HCl (pH 7.5), 1 mM EGTA, 0.1 mM EDTA, 3 mM NaN_3, and 0.1% BME with or without 150 mM NaCl added. Following freeze−thaw and low-speed centrifugation as in panel a, lipid-incorporated and unincorporated protein were analyzed by SDS−PAGE and Coomassie Blue staining and quantified. (c) Large phosphatidylserine liposomes (1 mg/mL total lipid) containing trace amounts of [^{125}I]TID-PC/16 were subjected to five cycles of rapid freeze−thaw with (freeze−thaw w. vinculin)- or without (freeze−thaw w/o. vinculin) 3 μM vinculin in 11.2 mM salt. Vinculin was then added to 3 μM to the liposomes frozen and thawed in the absence of protein. Vinculin and lipid were also incubated without freeze−thaw (no freeze−thaw). Samples were photolyzed as indicated and subjected to SDS−PAGE, and the radioactivity incorporated into the protein bands was determined. Background radioactivity measured in the same lane was always subtracted from that measured in the bands. Values represent the mean ± SD of three experiments. Hydrophobic labeling increases dramatically when vinculin and phospholipid are frozen and thawed together to drive formation of protein−lipid complexes.

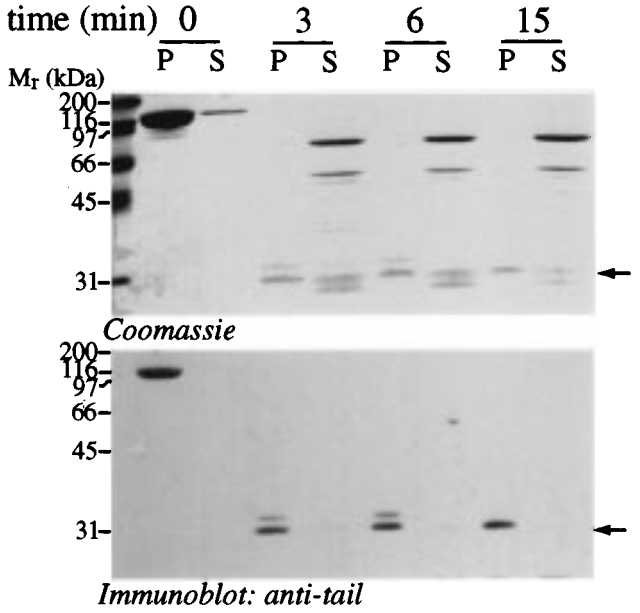

FIGURE 3: Lipid-bound vinculin is anchored by its carboxyl-terminal tail domain. PI-incorporated vinculin was isolated by freeze−thaw and low-speed centrifugation as in Figure 2a and resuspended in the same buffer. The sample was adjusted to protease V8 buffer [25 mM Tris-HCl (pH 7.6), 20 mM sodium acetate, 250 mM NaCl, 0.1 mM EDTA, and 1 mM EGTA] and digested at 37 °C with protease V8 (40 μg/mL). After digestion for 3 min, 4 mM PMSF was added to inhibit further proteolysis, and the reaction mixture was adjusted to approximately physiologic ionic strength (150 mM NaCl) by addition of H_2O. Aliquots were removed at the indicated times (time 0, start of V8 digestion) and centrifuged (12000*g* for 5 min) to recover PI vesicles. Pellet (P) and supernatant (S) fractions were analyzed by SDS−PAGE, followed by either Coomassie Blue staining (upper panel) or transfer to nitrocellulose and immunoblotting with a monoclonal antibody to the 30 kDa tail domain (lower panel). Within a few minutes of cleavage, the 30 kDa tail domain is the only fragment remaining associated with PI to a significant extent. The tail fragment remains bound to PI for several hours (data not shown).

The marked reduction in the salt sensitivity of vinculin−lipid association and enhanced hydrophobic photolabeling of vinculin during freeze−thaw suggested that proteolipid formation is mediated by the tail domain. This idea was examined by proteolytic analysis of lipid-incorporated vinculin. Vinculin was incorporated into PI vesicles by freeze−thaw and digested briefly with V8 protease, and proteolipid complexes were isolated by low-speed centrifugation at various times to determine what fragments of vinculin remain bound to the lipid vesicles. In a Coomassie-stained gel, only the 30 kDa tail domain fragment remains predominantly associated with PI throughout the time course (Figure 3, upper panel). A 32 kDa species, representing a tail fragment produced by V8 cleavage at amino acid (aa) residue 851 rather than at aa 857 (*17*), is also apparent. Immunoblot analysis using a monoclonal antibody recognizing the tail domain confirms the identity of these fragments (Figure 3, lower panel). These results demonstrate that the tail domain can function as an acidic phospholipid binding site in the context of the intact molecule during freeze−thaw. Because binding of the tail to the 95 kDa head domain blocks tail−lipid association (*6*), we hypothesize that the head−tail interaction in native vinculin is weakened by the rapid freezing and thawing used to drive proteoliposome assembly, transiently converting vinculin to an activated conformation in which the phospholipid binding site in the tail domain is exposed.

The Tail Domain of Vinculin Constitutes an Acidic Phospholipid Binding Module. The tail domain of vinculin is sufficient to direct the binding of an unrelated protein, glutathione *S*-transferase, to acidic phospholipids. A GST fusion protein containing vinculin residues 884−1066 (V884−1066) from the tail domain cosediments with PS and PI vesicles but not with PC vesicles, whereas GST itself does not cosediment with any of these lipids (Figure 4a). Thus, residues 884−1066 retain the same preference for acidic over neutral phospholipids observed with the native protein in gel filtration, cosedimentation, and hydrophobic photolabeling assays (*6*, *13*, *14*). These results indicate that phospholipid binding is a property of the amino acid sequence of the tail domain and not the result of potential lipid modifications of the protein (*34*, *35*), which would not occur in the bacterial expression system.

GST−V884−1066 is labeled by the hydrophobic probe [^{125}I]TID-PC/16 incorporated into PS vesicles, to an extent comparable to that observed with the 30 kDa tail fragment in low-ionic strength (11.2 mM salt) buffer (Figure 4b). GST−V884−1066 is also labeled at higher ionic strengths (95 mM salt); under these conditions, labeling of the 30 kDa tail is significantly reduced (Figure 4b), despite the fact that the 30 kDa fragment cosediments efficiently with lipid vesicles (Figure 1). Photolabeling is dependent upon acidic phospholipid; when the hydrophobic probe is incorporated into PC vesicles, specific labeling of GST−V884−1066 is less than 5% of that observed in the presence of PS (data not shown). Hydrophobic photolabeling of another GST−tail fusion protein spanning the tail domain, GST−V858−1066, can be blocked by preincubation with stoichiometric amounts of the 95 kDa head domain (Figure 4c), consistent with earlier findings that head−tail association masks the phospholipid binding ability of the tail (*6*), and providing further evidence that the head must be displaced from the tail before native vinculin can be inserted into acidic phospholipid bilayers. Overall, the data show that the lipid-associative properties of isolated V_t are expressed by the tail domain in vinculin once the intramolecular interaction of the head and tail is disrupted.

The efficiency of photolabeling of the tail domain in our hands is comparable to the efficiency of labeling of integral membrane proteins observed using similar photoactivatable probes. GST−V858−1066 maximally incorporates approximately 0.4% of the total probe radioactivity present, corresponding to 0.005 pmol of label bound per nanomole of protein. This compares favorably with values of 1.2% and 0.3−0.5% found, respectively, for band 3 and glycophorin, two erythrocyte integral membrane proteins (*32*). The low labeling efficiency obtained with photoactivatable reagents such as [^{125}I]TID-PC/16 is due to a predominant reaction of the photolysis-generated carbene intermediates with neighboring phospholipids (*32*).

Localization in the Tail Domain of a Minimal Sequence Sufficient for Binding and Insertion into Acidic Phospholipid Bilayers. We analyzed the phospholipid association and bilayer insertion potential of a series of truncation constructs of the tail domain (Figure 5a) by assaying both cosedimentation with PS vesicles (Figure 5b) and hydrophobic photolabeling (Figure 5c,d). GST−V884−1066 and GST−V858−1066, which contains all of the vinculin residues comprising the 30 kDa tail fragment, cosediment substantially and incorporate significant hydrophobic probe in both high- and low-ionic strength buffer, although in contrast to the 30

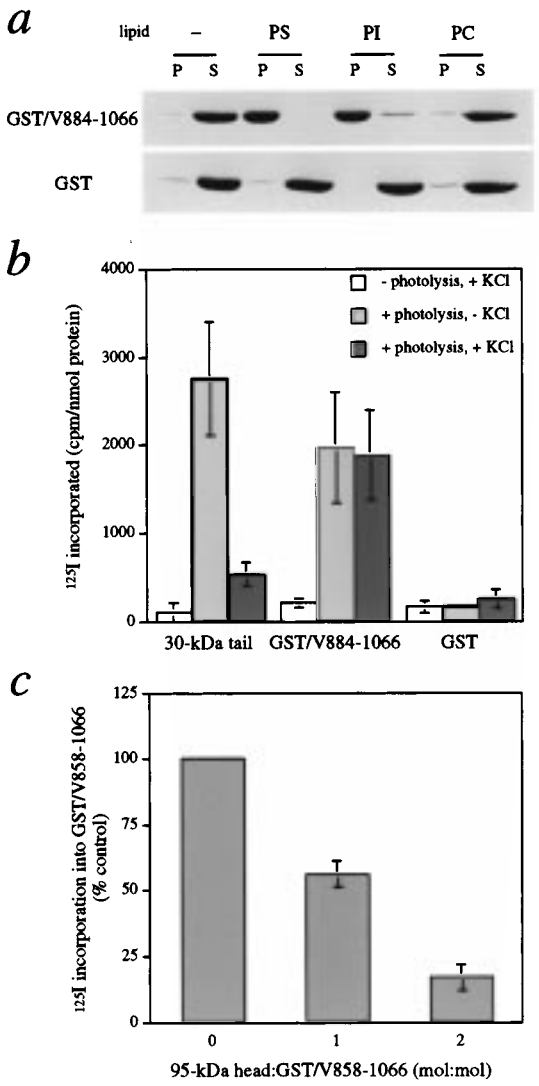

FIGURE 4: Vinculin tail domain and GST−tail fusion protein spontaneously bind and insert into acidic phospholipid vesicles in the absence of the head domain. (a) GST−V884−1066 or GST (2 μM) was incubated with the indicated phospholipids (0.5 mg/mL each) in buffer containing 95 mM salt. Vesicles were sedimented, and pellet (P) and supernatant (S) fractions were analyzed by SDS−PAGE and Coomassie Blue staining. The GST−tail fusion protein binds to both species of acidic phospholipid (PS and PI) but not to a neutral species (PC). GST itself does not bind phospholipid. (b) Purified 30 kDa tail (3.7 μM), GST−V884−1066 (3.3 μM), and GST (5.5 μM) were incubated with large phosphatidylserine liposomes containing trace amounts of [^{125}I]TID-PC/16, in the presence of 11.2 mM NaCl and in the absence or presence of 80 mM KCl. Samples were photolyzed and subjected to SDS−PAGE, and the radioactivity incorporated into the protein bands was determined. Background radioactivity measured in the same lane was always subtracted from that measured in the bands. Incorporated radioactivity is given as counts per minute per nanomole of protein. These data are the mean ± SD of three experiments. (c) GST−V858−1066 (2.5 or 5 μM) was preincubated (60 min at 22 °C) in the absence or presence of 95 kDa head fragment (5 μM), followed by addition of phosphatidylserine liposomes containing [^{125}I]TID-PC/16 and photolysis as described in Experimental Procedures. Reaction mixtures contained 80 mM KCl and 11.2 mM NaCl. Specific labeling in counts per minute per nanomole of protein was determined and is reported as the mean percent control labeling ± SD (n = 3). In the absence of head domain, GST−V858−1066 incorporated 3000−5000 cpm/nmol.

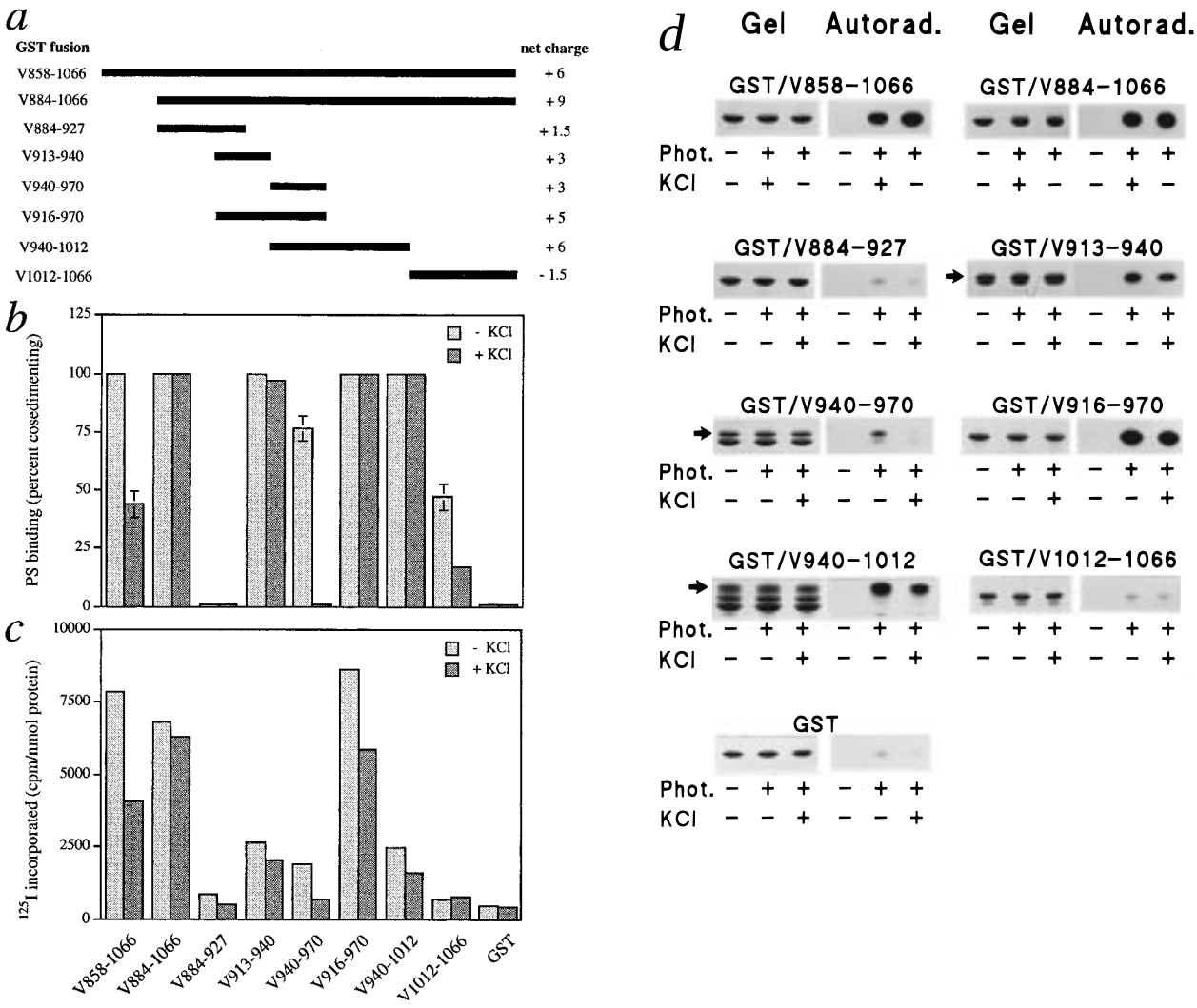

FIGURE 5: Vinculin residues 916−970 comprise the principal acidic phospholipid binding and insertion region in the tail domain. (a) Schematic outlining the regions from the vinculin tail expressed as GST−tail fusion protein constructs and used to map the sites of acidic phospholipid binding and hydrophobic probe labeling. The corresponding amino acid residue numbers from the chicken vinculin sequence are indicated on the left. Also shown is the expected net charge at neutral pH, counting basic residues as +1, acidic residues as −1, and histidine residues as +0.5. (b) The GST fusion proteins (2 μM) indicated on the horizontal axis of panel c were incubated with multilamellar PS vesicles, centrifuged, and subjected to SDS−PAGE as described in the legend of Figure 1. Reaction mixtures contained 15 mM NaCl with or without added 80 mM KCl as indicated. The percentage of total fusion protein which cosedimented with the PS vesicles is plotted as the mean ± SD of two determinations (error bars are not visible in all cases). In control samples, ≤5% of any of these fusion proteins sedimented in the absence of lipid (not shown). (c) GST−tail fusion proteins (3.3−5 μM intact species) were incubated with PS MLVs containing trace amounts of [^{125}I]TID-PC/16 in the presence of 11.2 mM NaCl with or without added 80 mM KCl as indicated. Following photolysis, an aliqout of each sample was applied to a 5 to 20% gradient gel. The radioactivity incorporated into the fusion protein bands was determined as described in Table 1. For GST−V940−1012 and GST−V940−970, specific incorporation into the intact band only was determined. Specific incorporation (in counts per minute per nanomole of protein) is plotted. (d) SDS−PAGE gels and corresponding autoradiograms from the experiment described in panel c. Phot. represents photolysis. Arrows indicate intact fusion protein species in cases where a substantial amount of breakdown products are present.

kDa tail fragment, binding of the V858−1066 construct to acidic phospholipids is partially sensitive to 95 mM salt. GST−V884−927 neither binds PS vesicles nor is inserted into PS bilayers, whereas GST−V913−940 and GST−V940−970 do, suggesting the presence of lipid binding sites in these latter two regions. Although the binding and labeling of GST−V913−940 are relatively insensitive to ionic strength, that of GST−V940−970 is abolished at 95 mM salt. However, binding and labeling of GST−V940−1012, another fusion protein spanning aa 940−970, is insensitive to ionic strength, suggesting that context may be important in determining ionic strength dependence.

Neither GST−V913−940 nor the two fusion proteins encompassing aa 940−970 are labeled by the hydrophobic probe to the same extent as the "full-length" tail constructs (GST−V858−1066 and GST−V884−1066) under the same conditions (Figure 5c). However, GST−V916−970, a fusion protein which encompasses both of these putative lipid binding sites, cosediments with PS vesicles in both high- and low-ionic strength buffers and is labeled by [^{125}I]TID-PC/16 to an extent comparable to that with the full-length constructs (Figure 5b,c). A GST fusion protein containing the carboxyl-terminal region of the tail, GST−V1012−1066, binds weakly to PS vesicles (Figure 5b). Positive charge is therefore not the sole determinant of phospholipid binding, since the anticipated net charge of V1012−1066 (−1.5) is more negative than that of V884−927 (1.5), a region which shows no detectable affinity for lipid, suggesting that

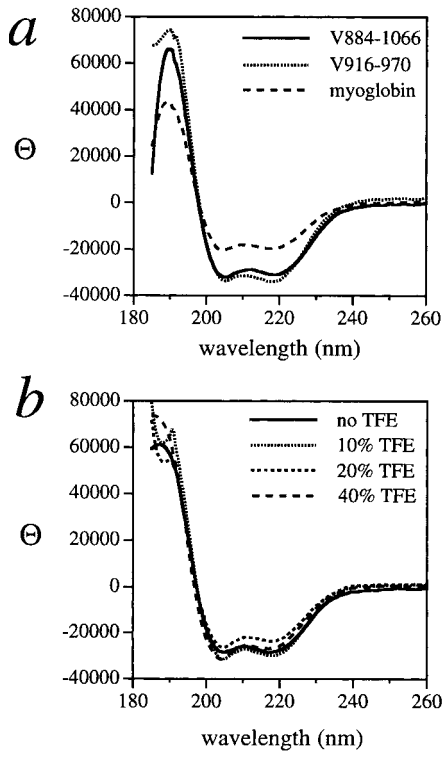

FIGURE 6: Circular dichroism analysis indicates a largely helical conformation for the lipid-binding site of vinculin. (a) CD spectra of V884−1066 (0.2 mg/mL), V916−970 (0.2 mg/mL), and horse heart myoglobin (0.22 mg/mL) in a physiological buffer [10 mM sodium phosphate (pH 7.0), 100 mM NaCl, 1 mM EDTA, 0.1 mM EGTA, 3 mM NaN_3, and 0.5 mM BME]. (b) CD spectra of 0.2 mg/mL V916−970 in buffer containing 0, 10, 20, or 40% TFE. The data are expressed as Θ, the mean residue ellipticity, which has units of deg cm^2 $dmol^{-1}$.

nonspecific electrostatic effects can be excluded. However, GST−V1012−1066 does not label significantly with the hydrophobic probe (Figure 5c,d). Thus, V916−970 is the only region which faithfully mimics the lipid binding and inserting properties of the intact tail. We conclude that the region comprising vinculin residues 916−970 contains two independent acidic phospholipid-binding sites which act together to mediate efficient acidic phospholipid association and bilayer insertion, thus accounting for both aspects of the interaction of the tail domain with acidic phospholipid bilayers.

Circular Dichroism Analysis Reveals a Subtantially Helical Character for the Phospholipid Binding Region of Vinculin. The region of the tail domain that acts as a phospholipid-binding site is likely to adopt an α-helical conformation, on the basis of the results of algorithms for secondary structure prediction (*36*−*38*). We measured the circular dichroism spectra of polypeptides corresponding to V884−1066 and V916−970, to verify the predicted secondary structure of these regions (Figure 6). To obtain the CD spectra of the vinculin regions in the absence of a fusion carrier such as GST, the V884−1066 and V916−970 regions were expressed in bacteria as His-tag fusion proteins, and separated from the His tag by proteolysis with thrombin. Circular dichroism spectra of the thrombin-cleaved proteins in a physiological buffer (see Experimental Procedures) were obtained.

The spectra of V884−1066 and V916−970 are very similar, each displaying two minima at 205−205.5 and 218−218.5 nm and a maximum at 189.5 nm (Figure 6a). The number and approximate position of these maxima and minima are consistent with a significant helical character for these polypeptides (*31*, *39*). We examined the spectral data using three algorithms (PROSEC, SELCON, and K2D) which utilize different approaches for deconvoluting CD data into secondary structure contributions (*39*−*42*). The results of these algorithms indicated a helical content of 60−90% for both V884−1066 and V916−970, although inspection of the fitted curves derived from the deconvolutions revealed a poor fit to the spectral data for both proteins (data not shown). The poor fit was most likely due to the fact that the maxima and minima in the spectra of helical proteins used as references by the deconvolution algorithms occur at 192 nm and at 208 and 222 nm, respectively; these values are significantly red-shifted relative to the corresponding values for V884−1066 and V916−970. The calibration of the spectropolarimeter we used was confirmed by measurement of the spectrum of (+)-10-camphorsulfonic acid (*31*). We conclude that the difference between our spectra and the reference helical spectra is due to differences in the experimental conditions employed. If the wavelength data for V884−1066 and V916−970 are manually edited so that the positions of the maxima and minima for these spectra match those of the reference spectra employed by the deconvolution algorithms, all three algorithms predict 90−100% helical character for both V884−1066 and V916−970, with a good fit, on the basis of visual inspection, between experimental and predicted spectra (data not shown).

We measured the CD spectrum of horse heart myoglobin, a protein which contains ∼80% helical secondary structure (*43*), to compare the spectrum of a known helical protein, obtained under our experimental conditions, with the spectra of V884−1066 and V916−970 (Figure 6a). In our hands, the maximum and minima in the spectrum of myoglobin were located at 189 nm and at 204.5 and 217.5 nm, respectively. The positions of these peaks, which are blue-shifted relative to those of the myoglobin spectra in the databases used by the deconvolution algorithms we employed, are essentially identical to the peak positions obtained for V884−1066 and V916−970, verifyng that these vinculin polypeptides adopt a largely α-helical conformation. Moreover, the magnitudes of the ellipticities at the maxima and minima in the V884−1066 and V916−970 spectra are greater than those of myoglobin, indicating that the vinculin polypeptides possess a higher helical content than does myoglobin. The spectrum of V916−970 is not significantly affected by addition of up to 40% TFE (Figure 6b), a compound which induces and stabilizes α-helical conformations in peptides (*44*), suggesting that the helical content of this region is stable and at a maximum. We conclude that V884−1066 and V916−970 adopt a highly (>80%) helical secondary structure under physiological buffer conditions.

Predicted Amphipathic Helices Comprise the Phospholipid-Binding Region. The CD analysis of V916−970 implies that most of the residues in this region, including the two lipid-binding sites, assume a helical conformation, as suggested by secondary structure prediction based on the amino acid sequence. A helical wheel projection of the two lipid-binding regions in V916−970 demonstrates their predicted amphipathicity, with one face enriched in hydrophobic residues and another face enriched in hydrophilic

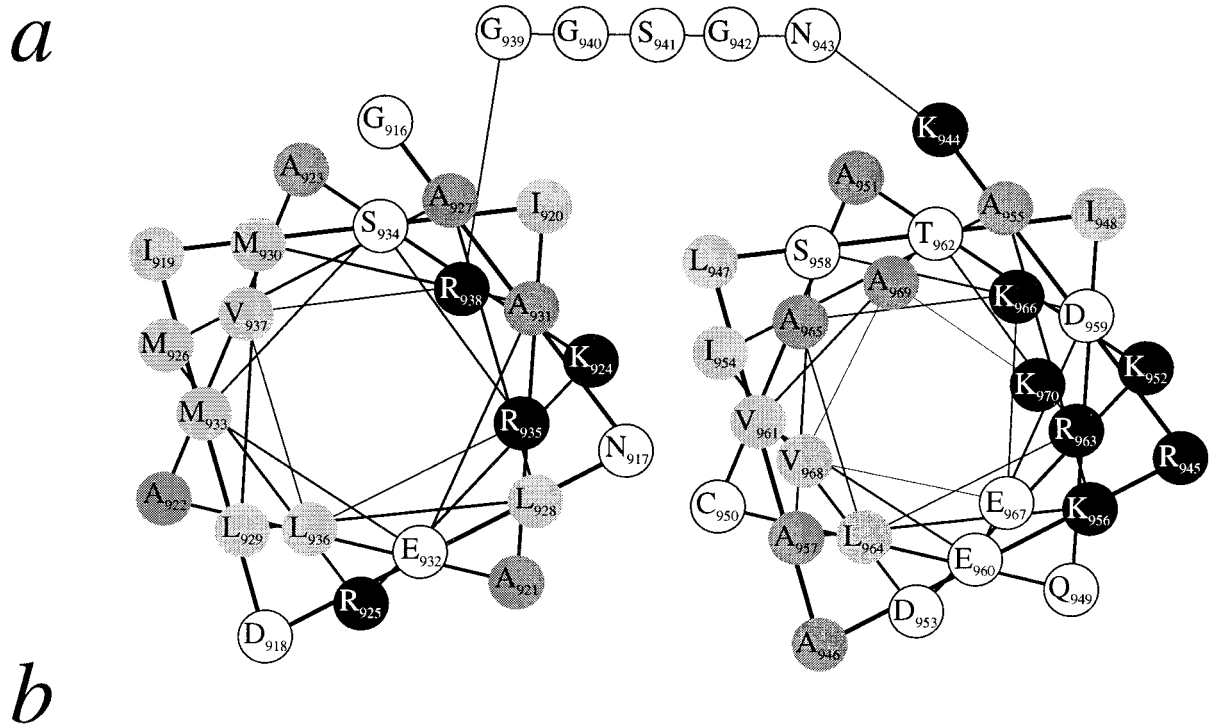

FIGURE 7: Tail domain residues 916−970 are predicted to form conserved amphipathic helices. (a) Secondary structure prediction algorithms (*36*−*38*) indicate that V916−970 contains two helical regions separated by a glycine-rich turn region. The predicted helices (V916−938 and V944−970) are projected onto two helical wheels separated by the glycine-rich segment. The helices are drawn so that their carboxyl termini project into the plane of the page. Residues are shaded according to the type of side chain: light gray, hydrophobic; black, basic; and dark gray, alanine. The helical wheel projection highlights the basic, amphipathic nature of these predicted helices. The high content of the helix-forming residue alanine is also apparent. (b) Alignment of V910−970 from the chicken vinculin sequence (vinc_Gg; *22*) with the homologous regions from nematode vinculin (vinc_Ce; *74*), *Drosophila* vinculin (vinc_Dm; FlyBase accession number X96601), and mouse α-catenin (acat_Mm; *45*). Shading highlights the high conservation (three out of four sequences) of the residues forming the hydrophobic faces of the two helices (light gray) and of several of the alanine residues (dark gray). Certain basic residues are also well-conserved (black), although the overall charge is not, particularly, between α-catenin and the vinculins. Conserved acidic residues are not shaded. The dark bars beneath the alignment identify the two lipid-binding subfragments (V916−940 and V940−970) of this region.

residues, particularly residues containing basic side chains (Figure 7a). Secondary structure prediction algorithms also suggest that a glycine-rich segment (aa 939−943) at the juncture of these two regions forms a turn separating the two amphipathic helices. The sequence of this phospholipid-binding region is conserved across several reported vinculin sequences, and between vinculin and the related protein α-catenin (*45*); the predicted helix−turn−helix structure is also retained between these proteins (Figure 7b and data not shown). Residues predicted to comprise the hydrophobic faces of the two helices are strongly conserved, as are specific basic residues. The predicted glycine-rich turn region is also conserved, with the α-catenin sequence containing another turn-promoting residue, proline, in addition to glycine. The overall positive charge of this region is not well-conserved between α-catenin and the vinculins, suggesting that only basic side chains at specific locations are critical.

DISCUSSION

The activation of phospholipid binding and insertion during freeze−thaw suggests that this process drives the opening of vinculin through disruption of the intramolecular head−tail interaction, allowing access of the phospholipid to its cryptic binding sites (*6*) on the tail even under physiologic ionic conditions. The level of hydrophobic photolabeling of vinculin observed in very low-ionic strength (e.g., no salt) buffers in earlier in vitro studies (*14*) is consistent with the salt-sensitive association of native vinculin with phospholipid and suggests that in the absence of freeze−thaw some fraction of the vinculin adsorbed to acidic phospholipid under these conditions is open and inserted into the bilayer. Thus, the data presented here provide direct evidence that intact vinculin can exist in two distinct conformational states, one with high affinity and one with low affinity for a target ligand, as previously proposed (*4*, *5*). Recent reinvestigation of the morphology of vinculin by refined electron microscopy techniques has provided images of the molecule that can be easily interpreted as open and closed forms of vinculin (*1*).

The increase in reactivity of vinculin during freze-thaw is not limited to phospholipid binding. Results from other studies in our lab indicate that binding of vinculin to other conformationally regulated ligands can also be enhanced by freeze−thaw (P. Steimle, N. Adey, and S. W. Craig, in

preparation). Although binding of ligands can be enhanced by freeze−thaw in the presence of vinculin, at present it is unclear whether the conformational change stimulated by freeze−thaw is only transient or stable in the absence of ligand. In the presence of a ligand such as phospholipid, the conformational change is clearly stabilized. This is apparent in Figure 3, where brief cleavage with V8 protease results in production of ∼75 and 30 kDa major fragments, rather than the 95 and 30 kDa fragments produced by cleavage of soluble vinculin (*18*), suggesting the PI-bound vinculin is in a conformation different from soluble vinculin. Changes in vinculin tryptic fragments in the presence of anionic phospholipids in low-ionic strength buffers were also observed in an earlier study (*13*). The mechanism by which freeze−thaw facilitates this conformational change in vinculin is also unknown, but may involve limited denaturation of regions of the protein which mediate the head−tail interaction. Limited denaturation with agents such as SDS has been observed to activate cryptic binding sites in ezrin, another protein whose ligand affinities are regulated by an intramolecular interaction (*46*).

An earlier in vivo study indicated that membrane-associated vinculin is inserted into the bilayer, since this pool of the protein is labeled by a photoactivatable fatty acid analogue after incorporation of the probe into cellular lipids (*16*). In contrast, vinculin isolated from the cytosolic fraction of the same cells was not labeled. In retrospect, these data suggest that vinculin associated with the plasma membrane in vivo is in an open conformation, thus supporting the proposal that vinculin recruitment to membrane sites such as focal adhesions involves, or leads to, activation of the molecule through disruption of the regulatory head−tail interaction (*4*, *5*). Activation of the molecule can be stimulated in vitro by physical and chemical perturbations such as proteolysis or freeze−thaw, but presumably, cellular factors control vinculin opening in vivo, to regulate where and when vinculin is activated during cellular processes.

Recently, two groups have reported evidence for acidic phospholipid-stimulated opening of vinculin in vitro (*8*, *9*). Of the various phospholipids tested, only PIP_2 and PIP displayed an ability to activate F-actin and talin binding by vinculin in one study (*8*), whereas the authors of the second report found that other acidic phospholipids such as PS, in addition to PIP_2, could stimulate vinculin binding to F-actin (*9*). These data suggest the formation of vinculin−lipid complexes in the physiologic ionic strength buffers used in the two studies; in contrast, our results indicate that native vinculin does not bind acidic phospholipid spontaneously under these conditions. Because activation of vinculin in the other reports was measured indirectly, by F-actin or talin binding assays, it is possible that these target proteins act cooperatively with acidic phospholipids to induce vinculin−lipid interaction in physiologic buffers; acidic phospholipids alone may not be capable of interacting with vinculin under physiologic conditions to mediate vinculin activation. The physical state in which acidic phospholipids are presented to vinculin in vitro in the various reports may also be significant. We have utilized MLVs in this work, whereas sonicated vesicles (presumably SUVs) and pure PIP_2 micelles (*9*) or mixed micelles with Triton X-100 (*8*) were used in the previous studies. SUVs and detergent micelles possess higher surface curvature than large vesicles such as MLVs; concomitant differences in lipid packing or accessibility of the hydrophobic interior between these lipid assemblies may affect the affinity or ionic strength dependence of vinculin association. This issue is of particular importance in light of our finding that vinculin activation by physical or chemical perturbation is correlated with enhanced hydrophobic insertion by the protein, suggesting that the ability to insert may be critical to activation. Similar effects of lipid presentation on phospholipid binding or lipid-stimulated enzyme activation have been noted in studies on other proteins, such as CTP:phosphocholine transferase (*47*) and protein kinase C (*48*, *49*). Further exploration of these issues is warranted in assessing the proposal that acidic phospholipids, particularly, PIP_2, regulate vinculin conformation in vivo (*8*, *9*).

Binding to Acidic Phospholipid Bilayers and Insertion into the Hydrophobic Core of the Bilayer Are Distinct Events with Different Structural Requirements. The photolabeling and cosedimentation data show that we can distinguish regions of the tail which physically associate with phospholipid and are inserted efficiently into the bilayer (e.g., V916−970) from regions which associate with lipid but are inserted less well (e.g., V913−940 and V940−970) or not significantly (V1012−1066). It is particularly striking that V916−970 mediates both efficient cosedimentation with phospholipid vesicles and photolabeling, while the two sites that comprise it, V913−940 and V940−970, each individually cosediment efficiently (at least at low ionic strengths) but label less well than V916−970. Although the carbene intermediate generated by the photoactivatable moiety of [^{125}I]TID-PC/16 displays some preference for sulfur-containing side chains, labeling of membrane-inserted polypeptides occurs at a variety of inserted aliphatic and aromatic amino acid residues (*32*), suggesting that quantitative differences in labeling observed between tail domain regions are meaningful. No region was identified which labeled with the photoactivatable probe but did not cosediment. These observations suggest that insertion of a fragment into the hydrophobic core is an event separate from adsorption to the phospholipid bilayer. Adsorption of a fragment to the surface of the bilayer is probably mediated by electrostatic interactions; depending on the properties of the adsorbed fragment, this surface binding is then stabilized by subsequent hydrophobic insertion. Taken together, these observations suggest that specific structural elements in the lipid-binding sites independently provide electrostatic and hydrophobic components to the interaction with acidic phospholipids.

Comparison with Other Lipid-Binding Motifs. The regions of the tail which contain phospholipid-binding sites are likely to form basic amphipathic α-helices, on the basis of circular dichroism analysis and the results of algorithms for secondary structure prediction. Indeed, V940−970 and V1012−1066 were identified by Tempel et al. (*50*) as probable lipid-binding sites solely on the basis of their predicted ability to form basic amphipathic helices. The two amphipathic helices in V916−970 are predicted to be separated by a glycine-rich turn. This hypothetical helical hairpin structure resembles the structure determined for the membrane insertion domain of diphtheria toxin (*51*, *52*), and is distinct from the β-sandwich structures determined by X-ray crystallography or NMR for the C2 domain (*53*) and for the PH and related PTB domains (*54*, *55*), distinct motifs which bind various

acidic phospholipids and inositol polyphosphates. By itself, the CD spectrum of V916−970 distinguishes this largely α-helical polypeptide from the predominantly β-sheet conformation of the C2 and PH domains. Phospholipid binding by the tail domain is also distinguished from lipid binding by these other motifs by the greater involvement of hydrophobic interactions. Lipid binding of PH domains appears to be mediated mainly by electrostatic and hydrogen-bonding interactions between basic residues in loop regions of the protein and the lipid headgroups (*54*−*57*), whereas tail association with phospholipid involves significant interaction with the acyl chains of the lipid.

A number of small, surface-active peptides such as mellitin (*58*) and mastoparan (*59*), and at least some of the presequences directing mitochondrial protein targeting (*60*, *61*), associate with phospholipid bilayers by adopting an amphipathic α-helical structure composed of one face rich in hydrophobic amino acids and another face rich in basic residues. This structure allows both insertion of the hydrophobic side chains into the fatty acyl core of the bilayer and interaction of the positively charged side chains with acidic lipid headgroups. Our analysis of the phospholipid binding site in vinculin indicates that it is a member of this class of lipid-binding motif. Other proteins such as the MARCKS protein (*62*), pp60^{src} (*63*), and some members of the Ras family (*64*) also bind to lipid through distinct bipartite motifs which utilize both electrostatic and hydrophobic interactions, although in all these cases covalent attachment of lipid to the protein is required to mediate hydrophobic interactions with membranes.

Talin and ezrin associate with acidic phospholipids through an amino-terminal domain which contains the region of homology defining the family of band 4.1-related proteins (*24*), suggesting that this module represents a conserved lipid-binding motif in a number of otherwise nonhomologous proteins. Talin and ezrin both bind several species of anionic phospholipids under various conditions in vitro, although polyphosphoinositides such as PIP_2 may be the preferred ligands under physiological ionic conditions (*24*, *65*, *66*). Like vinculin, talin is inserted into phospholipid bilayers (*24*). Further comparison of these lipid-binding sites with those of vinculin must await more refined mapping of the determinants of lipid binding in the band 4.1-like domains. We have detected no overall sequence homology or similar patterns of predicted secondary structure between the vinculin tail domain and the band 4.1-like regions of these proteins.

Sites that preferentially bind polyphosphoinositides have been identified in several cytoskeletal proteins, including gelsolin and related proteins (*67*), α-actinin (*68*), and profilin (*69*). These sites are composed of a short (≤20 aa) peptide stretch displaying a net positive charge and in some cases clusters of basic residues. Synthetic peptides corresponding to a PIP_2-binding site in gelsolin undergo a transition from a random coil to an amphipathic α-helical structure in the presence of PIP_2 or SDS, suggesting that, like V916−970, this gelsolin peptide forms electrostatic and hydrophobic interactions with acidic lipids (*70*). Profilin has not been observed to be inserted into lipid bilayers (*71*). Hydrophobic insertion of α-actinin has been detected (*72*), although it remains to be determined whether such insertion is mediated by the PIP_2-binding site or by other potential lipid-binding sites in this protein (*73*). Further structural characterization will help determine whether these polyphosphoinositide-binding peptides and the phospholipid-binding domain in vinculin represent similar lipid-binding motifs.

A Conserved Lipid-Binding Motif in the Vinculin/α-Catenin Family. Vinculin residues 916−970 account for the lipid binding properties of the tail domain. This region is conserved between vinculins from species widely separated on the phylogenetic tree, and is included in one of the homology blocks which define the vinculin/α-catenin family (*45*). In particular, the predicted amphipathic helices corresponding to the individual lipid-binding sites (V916−940 and V940−970 in chicken vinculin) are retained across the family, as is the glycine-rich turn, suggesting that this turn might be an important feature, perhaps for properly orienting the helices. These facts are consistent with the idea that this region represents a conserved acidic phospholipid-binding motif. This speculation is encouraged by the finding that the 447 carboxyl-terminal residues of murine α-catenin, which include this region of homology with the vinculin tail, mediate binding to PS and PI vesicles when expressed as a fusion with GST (R. P. Johnson and S. W. Craig, unpublished data). Further investigation will identify the specific side chains mediating contact with acidic phospholipids in this conserved motif. Identification of the specific residues mediating contact will be important in designing experiments for probing the function of vinculin−lipid and α-catenin−lipid interaction in cells.

ACKNOWLEDGMENT

We are grateful to Drs. Wolfgang Goldman and Gerhard Isenberg for stimulating this collaboration. We also thank K. Mujynya-Ludunge for excellent technical assistance; Prof. H. U. Keller, in whose department the labeling experiments were carried out, for continuous support; Dr. E. Sigel for helpful discussions; Dr. Paul Steimle for the His-tag V884−1066 fusion protein vector; Dr. S. Saga for anti-tail monoclonal antibody mAb 4.21; Drs. David Shortle and Jim Sinclair for help in using their spectropolarimeter; and Dr. M. Fechheimer for critical reading of the manuscript.

REFERENCES

1. Winkler, J., Lunsdorf, H., and Jockusch, B. M. (1996) *J. Struct. Biol. 116*, 270−277.
2. Reinhard, M., Rudiger, M., Jockusch, B. M., and Walter, U. (1996) *FEBS Lett. 399*, 103−107.
3. Goldmann, W. H., Ezzell, R. M., Adamson, E. D., Niggli, V., and Isenberg, G. (1996) *J. Muscle Res. Cell Motil. 17*, 1−5.
4. Johnson, R. P., and Craig, S. W. (1994) *J. Biol. Chem. 269*, 12611−12619.
5. Johnson, R. P., and Craig, S. W. (1995) *Nature 373*, 261−264.
6. Johnson, R. P., and Craig, S. W. (1995) *Biochem. Biophys. Res. Commun. 210*, 159−164.
7. Schwienbacher, C., Jockusch, B. M., and Rudiger, M. (1996) *FEBS Lett. 384*, 71−74.
8. Gilmore, A. P., and Burridge, K. (1996) *Nature 381*, 531−535.
9. Weekes, J., Barry, S. T., and Critchley, D. R. (1996) *Biochem. J. 314*, 827−832.
10. Janmey, P. A. (1994) *Annu. Rev. Physiol. 56*, 169−191.
11. Isenberg, G., and Goldmann, W. H. (1995) in *The Cytoskeleton, Vol. 1: Structure and Assembly*, pp 169−240, JAI Press, Inc., Greenwich, CT.
12. Newton, A. C. (1993) *Annu. Rev. Biophys. Biomol. Struct. 22*, 1−25.

13. Ito, S., Werth, D. K., Richert, N. D., and Pastan, I. (1983) *J. Biol. Chem. 258*, 14626−14631.
14. Niggli, V., Dimitrov, D. P., Brunner, J., and Burger, M. M. (1986) *J. Biol. Chem. 261*, 6912−6918.
15. Devaux, P. F. (1991) *Biochemistry 30*, 1163−1173.
16. Niggli, V., Sommer, L., Brunner, J., and Burger, M. M. (1990) *Eur. J. Biochem. 187*, 111−117.
17. Gimona, M., Small, J. V., Moeremans, M., Van Damme, J., Puype, M., and Vandekerckhove, J. (1988) *EMBO J. 7*, 2329−2334.
18. Groesch, M. E., and Otto, J. J. (1990) *Cell Motil. Cytoskeleton 15*, 41−50.
19. Weber, T., Paesold, G., Galli, C., Mischler, R., Semenza, G., and Brunner, J. (1994) *J. Biol. Chem. 269*, 18353−18358.
20. Feramisco, J. R., and Burridge, K. (1980) *J. Biol. Chem. 255*, 1194−1199.
21. Evans, R. R., Robson, R. M., and Stromer, M. H. (1984) *J. Biol. Chem. 259*, 3916−3924.
22. Coutu, M. D., and Craig, S. W. (1988) *Proc. Natl. Acad. Sci. U.S.A. 85*, 8535−8539.
23. Smith, D. B., and Johnson, K. S. (1988) *Gene 67*, 31−40.
24. Niggli, V., Kaufmann, S., Goldmann, W. H., Weber, T., and Isenberg, G. (1994) *Eur. J. Biochem. 224*, 951−957.
25. Evans, E., and Kwok, R. (1982) *Biochemistry 21*, 4874−4879.
26. Ames, B. N. (1966) *Methods Enzymol. 8*, 115−118.
27. Hogervorst, F., Admiraal, L. G., Niessen, C., Kuikman, I., Janssen, H., Daams, H., and Sonnenberg, A. (1993) *J. Cell Biol. 121*, 179−191.
28. Heise, H., Bayerl, T., Isenberg, G., and Sackmann, E. (1991) *Biochim. Biophys. Acta 1061*, 121−131.
29. Gill, S. C., and von Hippel, P. H. (1989) *Anal. Biochem. 182*, 319−326.
30. Crumpton, M. J., and Polson, A. (1965) *J. Mol. Biol. 11*, 722−729.
31. Johnson, W. C., Jr. (1990) *Proteins 7*, 205−214.
32. Brunner, J. (1993) *Annu. Rev. Biochem. 62*, 483−514.
33. Racker, E. (1979) *Methods Enzymol. 55*, 699−711.
34. Burn, P., and Burger, M. M. (1987) *Science 235*, 476−479.
35. Kellie, S., and Wigglesworth, N. M. (1987) *FEBS Lett. 213*, 428−432.
36. Chou, P. Y., and Fasman, G. D. (1974) *Biochemistry 13*, 222−245.
37. Garnier, J., Osguthorpe, D. J., and Robson, B. (1978) *J. Mol. Biol. 120*, 97−120.
38. Rost, B., and Sander, C. (1997) *J. Mol. Biol. 232*, 584−599.
39. Greenfield, N. J. (1996) *Anal. Biochem. 235*, 1−10.
40. Chang, C. T., Wu, C.-S. C., and Yang, J. T. (1978) *Anal. Biochem. 91*, 13−31.
41. Sreerema, N., and Woody, R. W. (1993) *Anal. Biochem. 209*, 32−44.
42. Andrade, M. A., Chacon, P., Merelo, J. J., and Moran, F. (1993) *Protein Eng. 6*, 383−390.
43. Evans, S. V., and Brayer, G. D. (1988) *J. Biol. Chem. 263*, 4263−4268.
44. Nelson, J. W., and Kallenbach, N. R. (1986) *Proteins 1*, 211−217.
45. Nagafuchi, A., Takeichi, M., and Tsukita, S. (1991) *Cell 65*, 849−857.
46. Gary, R., and Bretscher, A. (1995) *Mol. Biol. Cell 6*, 1061−1075.
47. Arnold, R. S., and Cornell, R. B. (1996) *Biochemistry 35*, 9917−9924.
48. Boni, L. T., and Rando, R. R. (1985) *J. Biol. Chem. 260*, 10819−10825.
49. Hannun, Y. A., Loomis, C. R., and Bell, R. M. (1986) *J. Biol. Chem. 261*, 7184−7190.
50. Tempel, M., Goldmann, W. H., Isenberg, G., and Sackmann, E. (1995) *Biophys. J. 69*, 228−241.
51. Choe, S., Bennett, M. J., Fujii, G., Curmi, P. M. G., Kantardjieff, K. A., Collier, R. J., and Eisenberg, D. (1992) *Nature 357*, 216−222.
52. Silverman, J. A., Mindell, J. A., Finkelstein, A., Shen, W. H., and Collier, R. J. (1994) *J. Biol. Chem. 269*, 22524−22532.
53. Sutton, R. B., Davletov, B. A., Berghuis, A. M., Sudhof, T. C., and Sprang, S. R. (1995) *Cell 80*, 929−938.
54. Harlan, J. E., Hajduk, P. J., Yoon, H. S., and Fesik, S. W. (1994) *Nature 371*, 168−170.
55. Zhou, M.-M., Ravichandran, K. S., Olejniczak, E. T., Petros, A. M., Meadows, R. P., Sattler, M., Harlan, J. E., Wade, W. S., Burakoff, S. J., and Fesik, S. W. (1995) *Nature 378*, 584−592.
56. Ferguson, K. M., Lemmon, M. A., Schlessinger, J., and Sigler, P. B. (1995) *Cell 83*, 1037−1046.
57. Hyvonen, M., Macias, M. J., Nilges, M., Oschkinat, H., Saraste, M., and Wilmanns, M. (1995) *EMBO J. 14*, 4676−4685.
58. Okada, A., Wakamatsu, K., Miyazawa, T., and Higashijima, T. (1994) *Biochemistry 33*, 9438−9446.
59. Wakamatsu, K., Okada, A., Miyazawa, T., Ohya, M., and Higashijima, T. (1992) *Biochemistry 31*, 5654−5660.
60. von Heijne, G. (1986) *EMBO J. 5*, 1335−1342.
61. Tamm, L. K. (1991) *Biochim. Biophys. Acta 1071*, 123−148.
62. McLaughlin, S., and Aderem, A. (1995) *Trends Biochem. Sci. 20*, 272−276.
63. Silverman, L., and Resh, M. D. (1992) *J. Cell Biol. 119*, 415−425.
64. Hancock, J. F., Paterson, H., and Marshall, C. J. (1990) *Cell 63*, 133−139.
65. Niggli, V., Andreoli, C., Roy, C., and Mangeat, P. (1995) *FEBS Lett. 376*, 172−176.
66. Isenberg, G., Niggli, V., Pieper, U., Kaufmann, S., and Goldmann, W. H. (1996) *FEBS Lett. 397*, 316−320.
67. Janmey, P. A., Lamb, J., Allen, P. G., and Matsudaira, P. (1992) *J. Biol. Chem. 267*, 11818−11823.
68. Fukami, K., Sawada, N., Endo, T., and Takenawa, T. (1996) *J. Biol. Chem. 271*, 2646−2650.
69. Sohn, R. H., Chen, J., Koblan, K. S., Bray, P. F., and Goldschmidt-Clermont, P. J. (1995) *J. Biol. Chem. 270*, 21114−21120.
70. Xian, W., Vegners, R., Janmey, P. A., and Braunlin, W. H. (1995) *Biophys. J. 69*, 2695−2702.
71. Macheskey, L. M., Goldschmidt-Clermont, P. J., and Pollard, T. D. (1990) *Cell Regul. 1*, 937−950.
72. Niggli, V., and Gimona, M. (1993) *Eur. J. Biochem. 213*, 1009−1015.
73. Meyer, R. K., Schindler, H., and Burger, M. M. (1982) *Proc. Natl. Acad. Sci. U.S.A. 79*, 4280−4284.
74. Barstead, R. J., and Waterston, R. H. (1989) *J. Biol. Chem. 264*, 10177−10185.

BI9727242